

Supporting information

1. Sample topography

Fig. S1 shows the typical topographic image of the sample after the rubbing processes in our experiments. We note that there is no detectable damage caused by tip although the roughness of the Si_3N_2 sample is only 1.3 nm. This implies that there were no permanent deformations on the sample.

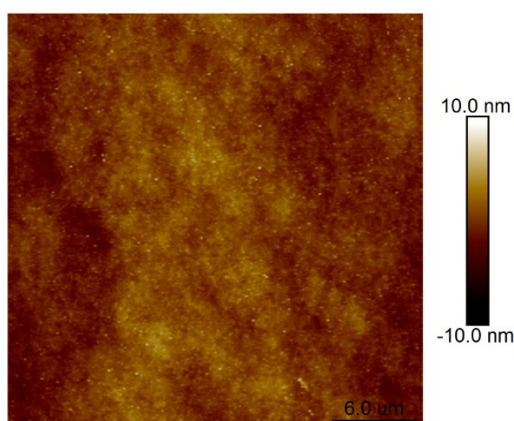


Figure S1. Typical topography of sample after rubbing processes

2. Effect of rubbing speed on charge transfer

Fig. S2 shows the observed charge transfer for various rubbing speeds. Here, no static contact was initiated at the beginning of the tracks. Further, the surface potential at beginning of the rubbing track only depended on the rubbing speed.

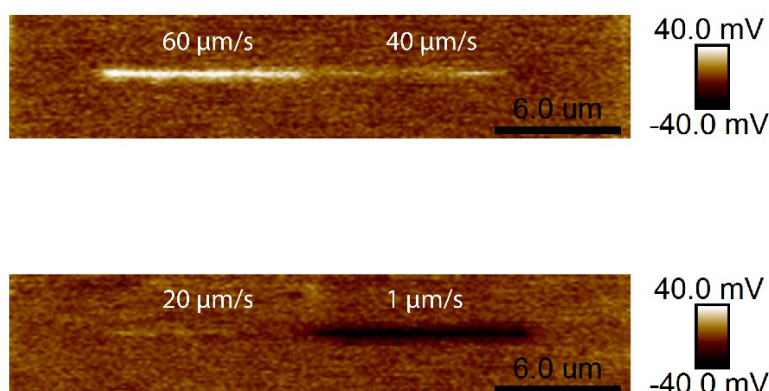


Figure S2. Polarity and magnitudes of transferred charge for various rubbing speeds.

3. Obtainment of accurate transferred charge values

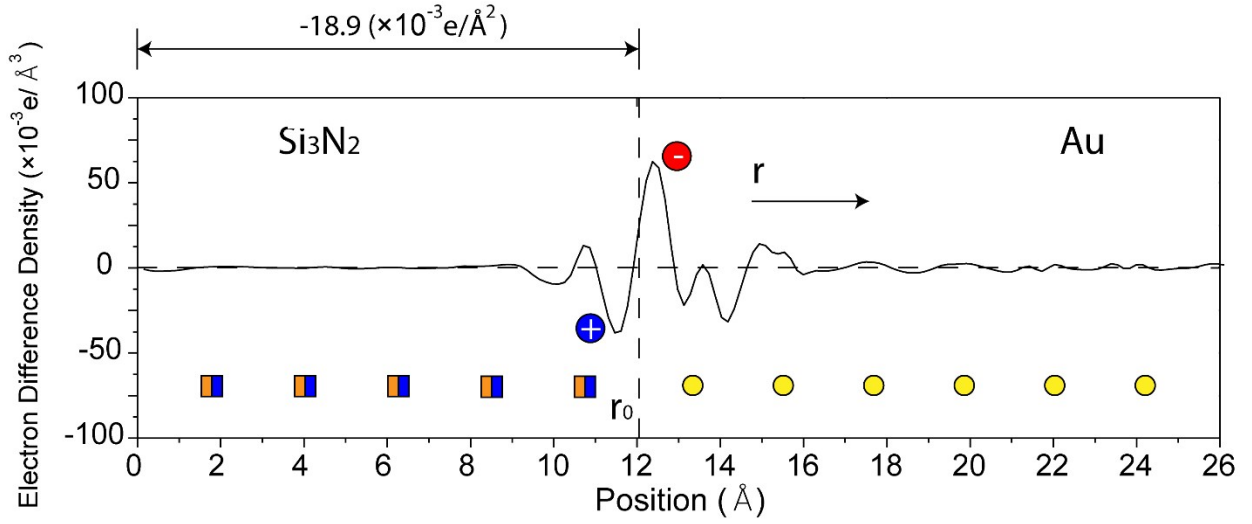


Figure S3. Calculation of transferred charge values.

Fig. S3 shows the plot of the EDD values as a function of the contact surface position. The transferred charge, calculated by integrating $\Delta\rho(r)$ from $-\infty$ to the node at r^0 between the Si_3N_2 and Au slabs, is expressed as Eq. S1.

$$q = e \int_{-\infty}^{r_0} \Delta\rho(r) dr \quad \text{S1}$$

Here, q , e , and $\Delta\rho(r)$ denote the transferred charge, charge of the electron, and EDD induced by the contact of Si_3N_2 slab and Au slab, respectively.

From Eq. S1, we calculated the transferred charge on the Si_3N_2 surface as $-18.9 \times 10^{-3} e/\text{\AA}^2$.

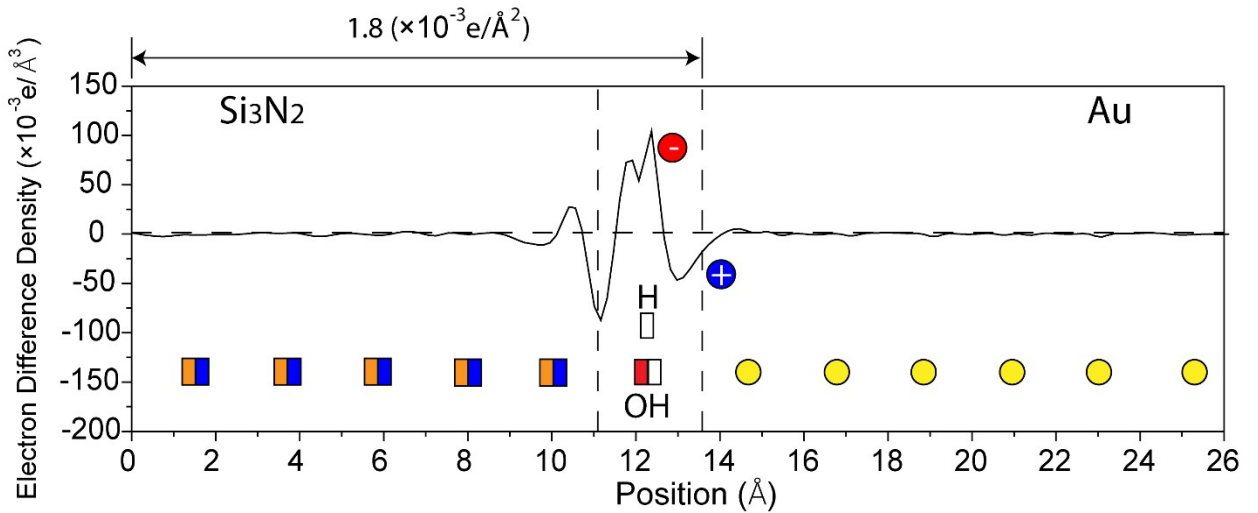


Figure S4. Calculation of transferred charge values with water present in the interface.

Similarly, the transferred charge on the Si_3N_2 surface was calculated as $1.8 \times 10^{-3} e/\text{\AA}^2$ with water present in the interface (Fig. S4).

4. The dissociation of H₂O on the interface between Au and Si₃N₂

When the geometry optimization is performed, the atom positions in the model will be fixed to reach the lowest energy. Here, the H₂O positions in the interface of Si₃N₂ and Au were optimized and four main locations of water molecules in the interface (Si-top, bridge, hollow, N-top) were considered. Figure S5 (a), (b), (c), and (d) show the geometries of water molecules on the Si-top, bridge, hollow and N-top position before optimization, respectively. Fig. S5 (e), (f), (g), and (h) show the geometries of water molecules on the Si-top, bridge, hollow and N-top position after optimization, respectively. We found that only the positions and directions of the water molecules were changed, when the oxygen atom of the water molecules locates on the Si-top, bridge, hollow positions of Si₃N₂ surface. Hence, it is physical adsorption when the oxygen atom in water molecule locates on these three positions. However, when the O atom of the water molecule locate on the N-top position of Si₃N₂ surface, the O atom and H atom will be attracted by different Silicon atoms on the Si₃N₂ surface. Under the attractions of different silicon atoms, the water molecule will be ripped and dissociated into an H atom and an OH radical after optimization as shown in Fig. S5 (h). And the H atom and OH radical were all bonding to silicon atoms according to further calculations.

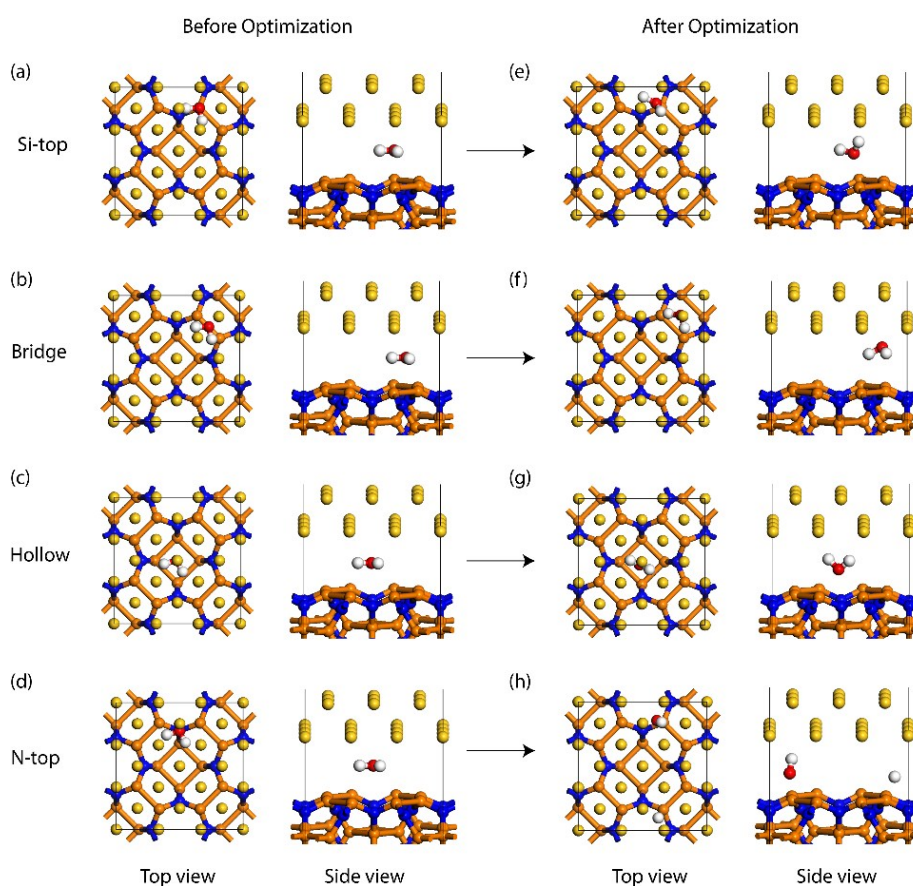


Figure S5. The initial geometries of H₂O on the Si-top, bridge, hollow and the N-top positions of Si₃N₂ surface and the optimized geometries

5. Effect of contact force on charge transfer

The contact forces, various from 10 nN to 110 nN, were applied on the tip when it rubbed the sample surface under 30 % and $25 \mu\text{m s}^{-1}$ rubbing speed. As shown in Fig. S6, the contact force can also affect both the polarity and magnitude of the transferred charge in triboelectrification. Increasing the contact load causes the surface potential to be more positive. It is suggested that the contact force may affect both the size of water meniscus and the contact area between the tip and the sample surface. Based on the calculations in this paper, the positive charges on the sample surface come from the tip, while the negative charges on the sample surface come from the water meniscus. Hence, a reasonable explanation is that increasing the contact force make the transferred charge more positive due to the increase of the contact area between the tip and the surface.

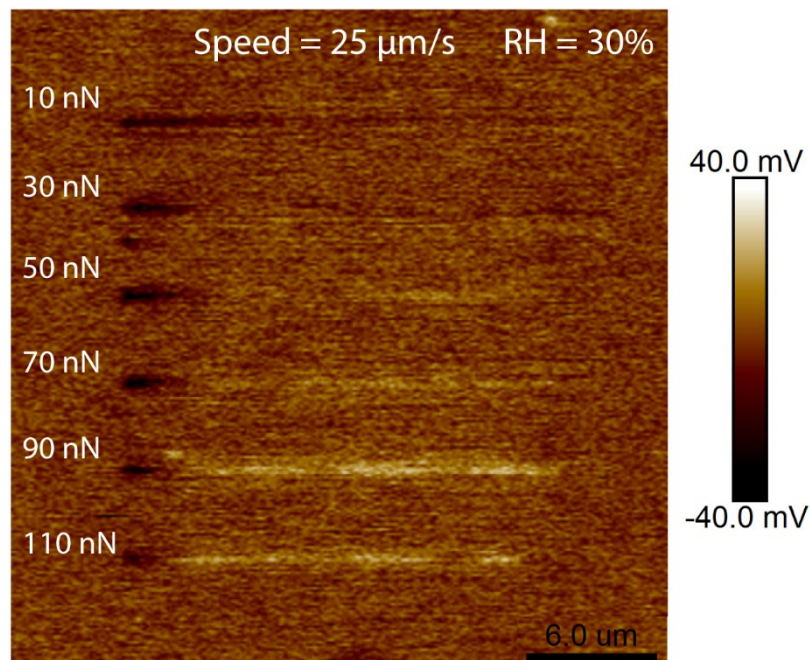


Figure S6. The effect of contact force on the triboelectrification

6. Difference charge transfer between regular AFM tip and micro sphere tip

A radius of $5 \mu\text{m}$ SiO_2 micro sphere was glued on the cantilever of a tip-less cantilever. Then, the tip and cantilever were coated with 50 nm Au by magnetron sputtering. The charge transfer between the micro sphere was studied with same method described in the manuscript, and the results are shown in Fig. S7. It is shown that the amount of transferred charge on the surface generated by the micro sphere tip is more positive than that with a regular tip. It indicates that the tip radius can affect the charge transfer. Based on our calculations, the positive charges on the sample surface come from the tip, while the negative charges on the sample surface come from the water meniscus.

Hence, the polarity and magnitude of transferred charge is depended on the competition between the contact area (tip and sample surface) and the size of meniscus. Increasing tip radius leads to larger contact area. Therefore, it is reasonable that the surface are more positive with the micro sphere tip than with the regular tip.

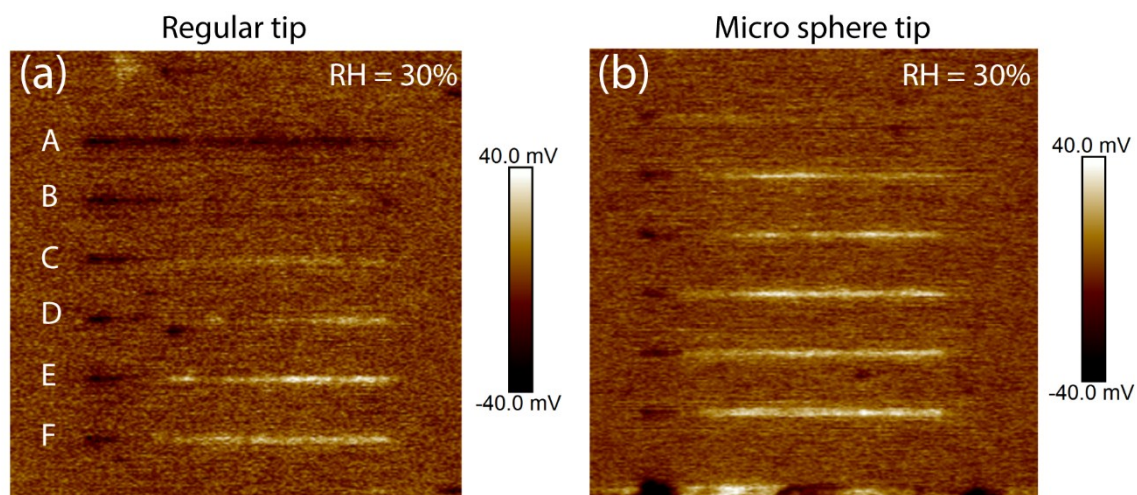


Figure S7. Difference of regular AFM tip and micro sphere tip in charge transfer